

Rotating patterns in polariton condensates in ring-shaped potentials under bichromatic pump

YAROSLAV V. KARTASHOV^{1,2} AND DMITRY A. ZEZYULIN^{3,*}

¹Institute of Spectroscopy, Russian Academy of Sciences, Troitsk, Moscow, 108840, Russia

²Russian Quantum Center, Skolkovo 143025, Russia

³ITMO University, St. Petersburg 197101, Russia

*Corresponding author: dzezyulin@itmo.ru

Compiled February 1, 2022

We consider a polariton condensate in a microcavity driven by a bichromatic resonant pump formed by two vortical laser beams carrying different topological charges. The system is additionally confined in a ring-shaped potential. We show that in this system steadily rotating nonlinear localized modes can be excited, whose angular rotation frequency is determined by optical frequencies and topological charges of the pump beams. When pump frequencies approach eigenfrequencies of the modes of the ring potential, resonant growth of peak amplitude of the excited states occurs. Repulsive polariton-polariton interactions lead to tilting of the resonance curves and appearance of bistability of rotating patterns. © 2022 Optical Society of America

OCIS codes: (190.5940) Self-action effects; (190.6135) Spatial solitons.

<http://dx.doi.org/10.1364/ao.XX.XXXXXX>

Cavity polaritons are bosonic quasiparticles that emerge in the regime of the strong coupling between the excitonic resonance and the photonic mode of the planar semiconductor microcavity [1]. The presence of the excitonic component results in strong polariton-polariton interactions, giving rise to various nonlinear effects and enabling Bose-Einstein condensation of polaritons. Characteristic feature of the polariton condensate is its inherently non-equilibrium nature due to photon leakage from the microcavity and recombination processes. A quasi-stationary regime can be achieved in the presence of the external pump, which can be resonant or non-resonant. In the former case, the properties of the excited patterns and excitation efficiency strongly depend on the pump shape/frequency and microcavity structuring, leading to appearance of the confining potentials.

Polariton condensates were used to demonstrate a variety of nonlinear patterns, including oblique dark [2–6] and bright [7] solitons. Superfluid nature of polariton condensates [8] enables a host of associated phenomena, such as persistent currents [9, 10], Bogoliubov-like spectrum of excitations [11], azimuthal solitons [12], multipole solitons [13], polygon patterns [14], and nucleation of vortices [10, 15–20] and vortex molecules [21] carrying quantized topological charges. Nucleation of polar-

ton vortices can be controlled by incoherent [15, 22–25] or coherent [10, 26, 27] pump. The presence of the confining potentials, which can be created using controllable metallization [28], etching [29] or other techniques [30] of microcavity structuring, substantially facilitates the formation of excitations with desired symmetries.

Most of the works on coherently pumped polariton condensates utilize single pump beam with certain optical frequency. Formation of spontaneous extended patterns excited by two broad pump beams from the external lasers has been considered only in uniform microcavities [31]. Thus, the interplay of the bichromatic pump and structuring of the microcavity remains largely unexplored.

The goal of this Letter is to describe rich resonant phenomena emerging in the presence of *bichromatic* pump in the microcavity with ring-shaped potential. We consider pump beams carrying different topological charges and show that such a pump, when it is resonant with eigenmodes of ring potential, leads to excitation of steadily rotating states with nontrivial phase distributions, whose rotation frequency is determined by the optical frequencies and topological charges of the pump beams. We also discuss bistability effects appearing due to repulsive nonlinearity in polariton condensate and leading to co-existence of several stable rotating patterns.

To model evolution of the polariton condensate in a planar microcavity under bichromatic pump, we use dimensionless Gross-Pitaevskii equation:

$$i\partial_t \psi = \left[-\frac{1}{2} \nabla^2 + V(r) - i\gamma + |\psi|^2 \right] \psi + \mathcal{H}(x, y, t), \quad (1)$$

where $\psi(x, y, t)$ is the complex-valued macroscopic wavefunction of the condensate, $\nabla^2 = \partial_x^2 + \partial_y^2$ is the Laplacian, time t and spatial coordinates x, y . The ring-like potential of depth V_0 is described by the function $V(r) = -V_0[e^{-(r-r_0)^2/w^2} + e^{-(r+r_0)^2/w^2}]$ ensuring smoothness of the potential at $r = 0$, where $r = (x^2 + y^2)^{1/2}$ is the polar radius, r_0 is the radius of the ring and w is its width. The parameter γ accounts for polariton losses. The function $\mathcal{H}(x, y, t)$ describes bichromatic pump by two laser beams with integer topological charges $m_{1,2}$ and frequency detunings $\epsilon_{1,2}$: $\mathcal{H} = h_1 S_1(r) e^{im_1 \phi - i\epsilon_1 t} + h_2 S_2(r) e^{im_2 \phi - i\epsilon_2 t}$, where $h_{1,2}$ are the pump amplitudes, $S_{1,2}(r) = r^{|m_{1,2}|} e^{-r^2}$ are the functions describing azimuthally symmetric pump profiles, and ϕ is the po-

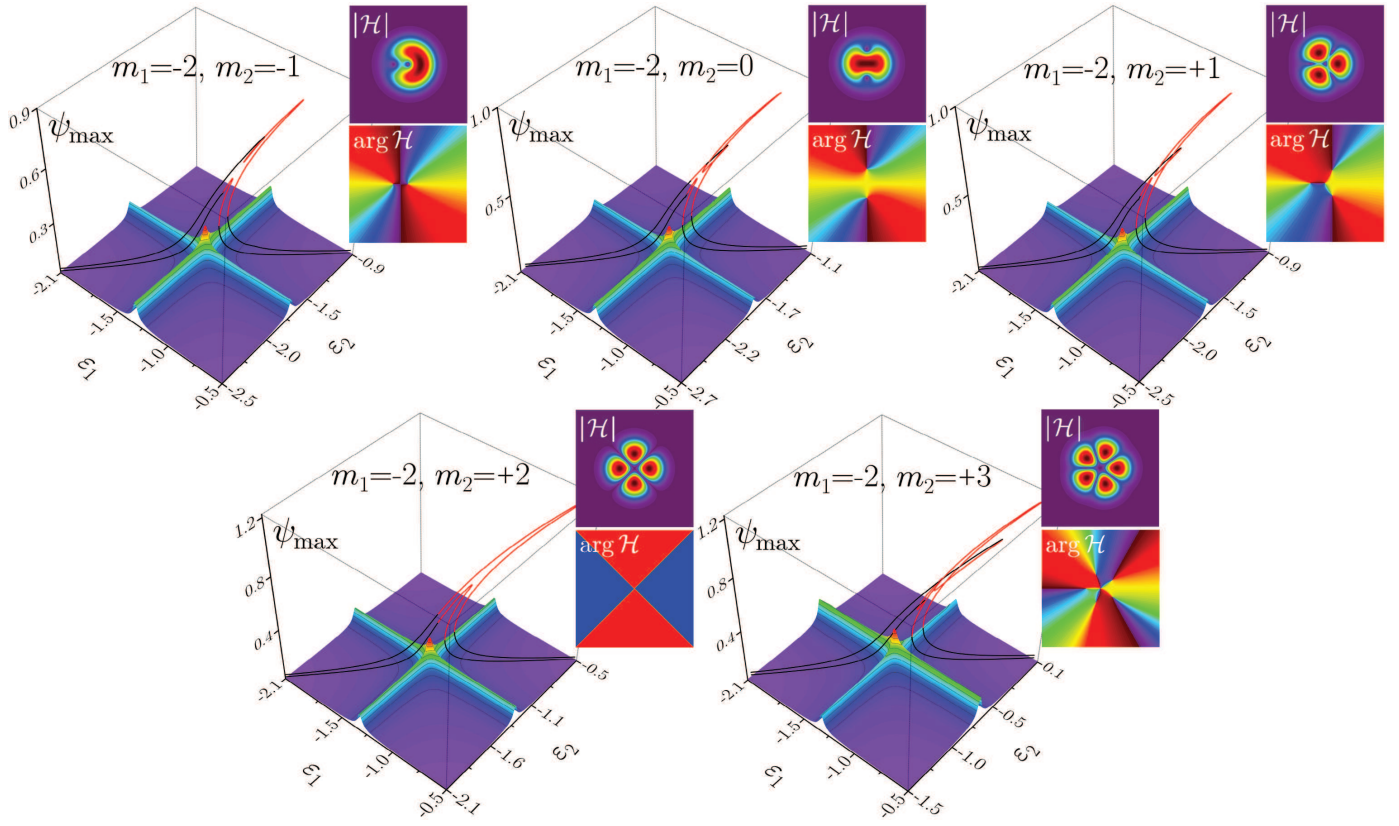


Fig. 1. 2D surface plots illustrate linear resonance dependencies $\psi_{\max}(\epsilon_1, \epsilon_2)$ at $h_{1,2} = 0.02$ for different combinations of topological charges of the pump $m_{1,2}$. Insets show corresponding pump modulus and phase distributions at $t = 0$. Lines above surface plots show nonlinear resonance curves $\psi_{\max}(\delta)$ calculated along the diagonal in the (ϵ_1, ϵ_2) plane passing through linear resonance point for selected topological charges $m_{1,2}$. Nonlinear resonance curves are shown for $h_{1,2} = 0.05$ and $h_{1,2} = 0.10$. Stable branches are shown black, unstable branches are shown red.

lar angle. Equation (1) also accounts for repulsive interactions between polaritons. In order to map dimensionless Eq. (1) to typical physical units, we assume the effective polariton mass $m \approx 10^{-34}$ kg and the unit length $\ell = 1 \mu\text{m}$. Then the dimensionless time unit in Eq. (1) corresponds to $\tau = m\ell^2/\hbar \approx 1 \text{ ps}$. The characteristic energy $\hbar^2/m\ell^2$ corresponding to one dimensionless unit of potential depth is $\approx 0.7 \text{ meV}$.

Since bichromatic pump contains two different frequencies, the existence of steady-state modes is not obvious apriori. To show that they can exist, we move into rotating coordinate frame $x' = x \cos(\omega t) + y \sin(\omega t)$, $y' = y \cos(\omega t) - x \sin(\omega t)$, where ω is the angular rotation frequency, and where Eq. (1) reads as:

$$\begin{aligned} i\partial_t \psi &= \left[-\frac{1}{2}(\partial_{x'}^2 + \partial_{y'}^2) + V(r) - i\gamma + |\psi|^2 \right] \psi \\ &+ i\omega(x' \partial_{y'} - y' \partial_{x'})\psi + h_1 S_1(r) e^{im_1 \phi' - i\epsilon'_1 t} + h_2 S_2(r) e^{im_2 \phi' - i\epsilon'_2 t}, \end{aligned} \quad (2)$$

where $V(r)$ and $S_{1,2}(r)$ do not change, since they do not depend on polar angle, ϕ' is the polar angle in the rotating frame, $\epsilon'_{1,2} = \epsilon_{1,2} - m_{1,2}\omega$ are pump frequency detunings in the rotating frame, and additional Coriolis term $i\omega(x' \partial_{y'} - y' \partial_{x'})\psi$ appears. Steadily rotating states of the form $\psi = u(x', y')e^{-i\mu t}$ are possible in Eq. (2) if all quantities evolve in time with the same rate $\epsilon'_1 = \epsilon'_2 = \mu$, where μ has the meaning of the effective

energy. This determines the rotation frequency of the pattern:

$$\omega = (\epsilon_1 - \epsilon_2)/(m_1 - m_2). \quad (3)$$

that depends on both detunings $\epsilon_{1,2}$ and topological charges $m_{1,2}$ of the pump, as well as effective energy:

$$\mu = (m_1 \epsilon_2 - m_2 \epsilon_1)/(m_1 - m_2). \quad (4)$$

The most representative feature of the resonant pump is that the amplitude of the modes that it excites resonantly increases when frequency of the pump approaches eigenfrequencies of corresponding linear eigenmodes of the system. Moreover, efficient excitation of such modes requires matching of their topological charge with topological charge of the pump. Our ring-like potential $V(r)$ supports finite number of localized modes with different topological charges that can be found from eigenvalue problem $\mu_m u_m = [-(1/2)\nabla^2 + V(r)]u_m$ obtained from linear version of Eq. (1) at $\gamma = 0$, where μ_m and u_m are the eigenfrequency and eigenmode profile corresponding to topological charge m . For representative depth $V_0 = 6$, width $w = 0.25$, and radius $r_0 = 2$ that we use here, the ring-like potential supports four modes with eigenfrequencies $\mu_0 = -1.865$, $\mu_{\pm 1} = -1.719$, $\mu_{\pm 2} = -1.312$, and $\mu_{\pm 3} = -0.676$, three of which are degenerate, because they correspond to opposite values of topological charge m . When pumping simultaneously at two frequencies in linear system one excites combinations of two modes with topological charges dictated by the pump, whose interference

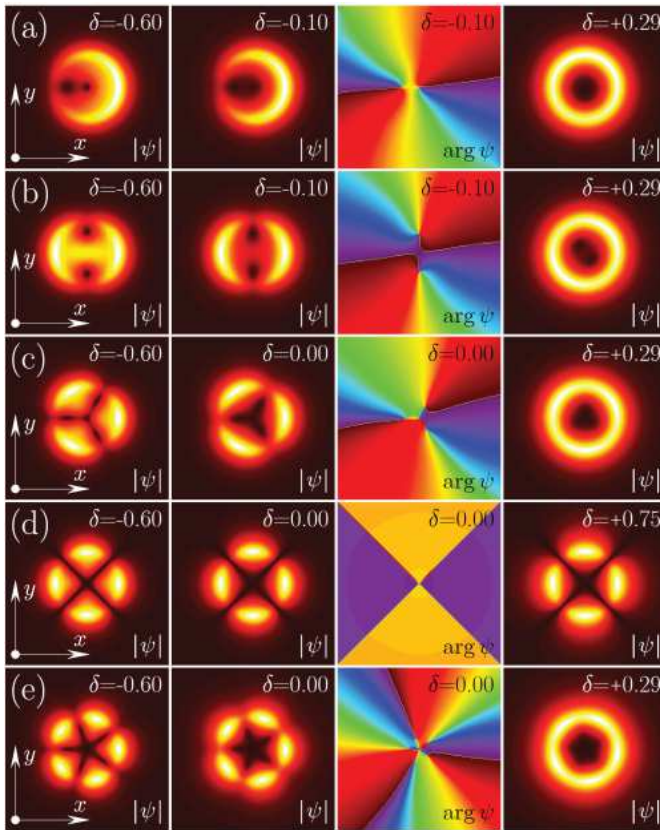


Fig. 2. Examples of modulus distributions of polariton wavefunction ψ at $h_{1,2} = 0.1$ for different values of detuning δ and different combinations of topological charges of the pump components: (a) $m_2 = -1$, (b) $m_2 = 0$, (c) $m_2 = +1$, (d) $m_2 = +2$, (e) $m_2 = +3$, while $m_1 = -2$ in all cases. All states are taken from the “upper” branch that smoothly continues to large negative δ values. Third column shows phase distributions $\arg \psi$ corresponding to $|\psi|$ distribution from the second column. All plots are shown in $x, y \in [-5, 5]$ window.

results in patterns rotating with the frequency (3). The weight of each mode in superposition depends on how close is pump frequency $\varepsilon_{1,2}$ to the eigenfrequency of this mode. The dependence of the maximal amplitude $\psi_{\max} = \max|\psi|$ of resulting rotating pattern on ε_1 and ε_2 in the linear case is shown in the form of 2D surfaces in Fig. 1 for five different combinations of the topological charges in the pump components (further we set $m_1 = -2$ and gradually increase m_2) and equal pump amplitudes $h_1 = h_2$. Each surface involves two perpendicular crests, which emerge at ε_1 and ε_2 values coinciding with eigenfrequencies μ_{m_1} and μ_{m_2} of the modes of the potential. Their intersection produces a spike, where two modes interfere with maximal amplitudes, that corresponds to the case when both pump frequencies are in resonance with eigenmodes of the potential. Like for any driven dissipative system, the height of the spike decreases with γ (hereafter we use typical for polaritons value of losses $\gamma = 0.02$).

In the presence of nonlinearity resonances become asymmetric: they tilt progressively toward larger $\varepsilon_{1,2}$ values with increase of pump amplitude $h_{1,2}$, so that at one point bistability emerges. To demonstrate this effect we scan the parameter plane $(\varepsilon_1, \varepsilon_2)$ along the diagonal passing through linear res-

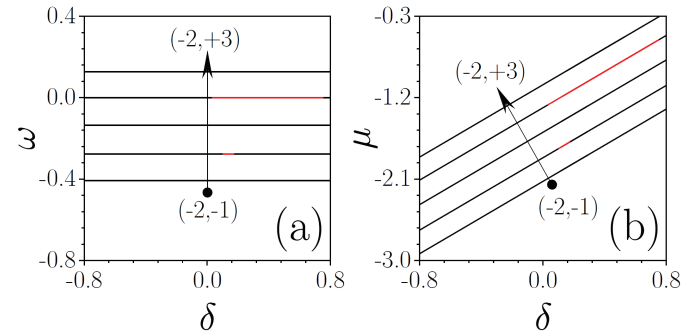


Fig. 3. Effective rotation frequency (a) and energy (b) vs. detuning δ for diagonal scan on the $(\varepsilon_1, \varepsilon_2)$ plane and for different combinations of topological charges (m_1, m_2) in the pump. In all cases $m_1 = -2$, while direction of increase of m_2 from -1 to +3 is shown by arrows. Red segments correspond to detuning intervals, where upper branch is unstable at $h_{1,2} = 0.10$.

onance at $\varepsilon_1 = \mu_{m_1}$ and $\varepsilon_2 = \mu_{m_2}$. We thus introduce and change the parameter δ — frequency detuning from linear resonance — such that pump frequencies vary as $\varepsilon_1(\delta) = \mu_{m_1} + \delta$ and $\varepsilon_2(\delta) = \mu_{m_2} + \delta$. Calculated *nonlinear* resonance curves $\psi_{\max}(\delta)$ for two different amplitudes of the bichromatic pump are shown with solid lines on top of 2D surfaces in Fig. 1. Progressively increasing nonlinearity-induced tilt of resonances leading to coexistence of several solutions is obvious. For $h_{1,2} = 0.10$ the upper branch (that can be smoothly continued to large negative δ values) tends to create a loop, that leads to coexistence of five states, for $h_{1,2} = 0.05$ up to three states can coexist for the same δ . The symmetry of corresponding rotating states is determined by the topological charges of the pump, see Fig. 2. For negative and zero detuning δ all shown patterns from the upper branch feature distinctive multipole shapes with nontrivial phase distributions with several nested vortices (see third column of Fig. 2) and the number of “petals” equal to $|m_1 - m_2|$, in agreement with pump modulus distribution $|\mathcal{H}|$ (see insets in Fig. 1). However, with increase of δ to sufficiently large positive values in all such states nested vortices move to the center and the pattern becomes nearly ring-like (see fourth column of Fig. 2), with the only exception for state generated by $m_1 = -2$, $m_2 = +2$ pump that does not rotate for detuning values taken from the diagonal on the $(\varepsilon_1, \varepsilon_2)$ plane (if one moves along any other line in this plane this state also transforms into ring-like structure). Substituting $\varepsilon_1 = \mu_{m_1} + \delta$ and $\varepsilon_2 = \mu_{m_2} + \delta$ into Eqs. (3) and (4), one obtains the following expressions for rotation frequency and energy: $\omega = (\mu_{m_1} - \mu_{m_2})/(m_1 - m_2)$, $\mu = \delta + (m_1 \mu_{m_2} - m_2 \mu_{m_1})/(m_1 - m_2)$, i.e., when we move along the diagonal in the $(\varepsilon_1, \varepsilon_2)$ plane, the rotation frequency of the pattern does not change, while energy changes linearly with δ . These simple observations are illustrated in Fig. 3.

Stability of the rotating states is determined by the pump amplitude $h_{1,2}$ and detuning δ . To test stability, we have employed the standard approach based on the linearization [32] of Eq. (1) with respect to small perturbation of a steadily rotating state. The outcome of the linear stability analysis have been also confirmed by the direct solution of Eq. (1) with initial conditions corresponding to slightly perturbed rotating states. The results of the stability analysis are indicated on the nonlinear resonance

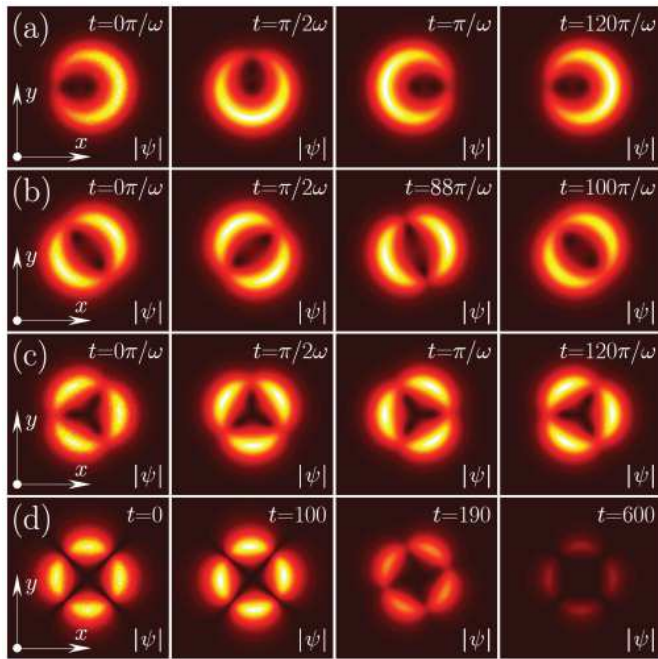


Fig. 4. Examples of stable evolution of the rotating states at $\delta = -0.1$, $m_2 = -1$ (a) and $\delta = 0$, $m_2 = +1$ (c). (b) Instability development at $\delta = +0.1$, $m_2 = 0$ leading to formation of persistent breather with the period $\approx 22.6\pi/\omega$. (d) Instability development leading to switching of the state from the upper to lower branch at $\delta = +0.29$, $m_2 = +2$. In (a),(c), and (d) pump amplitude $h_{1,2} = 0.10$, while in (b) $h_{1,2} = 0.05$. All input states are taken from the upper branch that smoothly continues to negative δ values. All distributions are shown within $x, y \in [-5, 5]$ window. See [Visualizations 1,2,3,4](#).

curves in Fig. 1, where black and red segments correspond, respectively, to stable and unstable states. Lower branches are always stable, upper branches are usually stable up to the critical value of δ (typically corresponding to the point, where this branch starts to make a loop), and middle branches are unstable. Examples of persistent rotation of perturbed modes from stable portions of the upper branch are presented in Figs. 4(a,c). These modes do not change their symmetry over multiple rotation cycles. Unstable modes show different scenarios of instability development. Close to the critical value of δ , where instability emerges, one observes formation of persistent breathers (states with oscillating peak amplitude) with periods far exceeding rotation period [see Fig. 4(b) where reorientation of the pattern, accompanying amplitude breathing, is obvious from last two columns]. Unstable states close to the tip of the resonance curve usually switch to small-amplitude stable state from the lower branch, sometimes after slight initial reorientation, see Fig. 4(d). Stable rotating patterns are attractors that can emerge from the input having very distinct shape — in the course of evolution they start rotating with the frequency given by Eq. (3).

To conclude, we have demonstrated that polariton microcavity with ring-like potential in the presence of bichromatic resonant pump supports a variety of rotating stable states, whose spatial shape and rotation frequency are fully determined by the topological charges and frequencies of the pump beams. Experimental relevance of our findings is confirmed by the fact

that rotating vortices driven by pulsed resonant excitation have been already observed in polariton condensates in the noninteracting regime [33].

FUNDING INFORMATION

Russian Science Foundation (Project 17-12-01413).

REFERENCES

- H. Deng, H. Haug, and Y. Yamamoto, Rev. Mod. Phys. **82**, 1489 (2010).
- A. Amo, S. Pigeon, D. Sunvitto, V. G. Sala, R. Hivet, I. Carusotto, F. Pisanello, G. Lemenager, R. Houdre, E. Giacobino, C. Ciuti, and A. Bramati, Science **332**, 1167 (2011).
- A. V. Yulin, O. A. Egorov, F. Lederer, and D. V. Skryabin, Phys. Rev. A **78**, 061801(R) (2008).
- Y. Xue and M. Matuszewski, Phys. Rev. Lett. **112**, 216401 (2014).
- V. Goblot, H. S. Nguyen, I. Carusotto, E. Galopin, A. Lemaître, I. Sagnes, A. Amo, and J. Bloch, Phys. Rev. Lett. **117**, 217401 (2016).
- L. A. Smirnov, D. A. Smirnova, E. A. Ostrovskaya, and Yu. S. Kivshar, Phys. Rev. B **89**, 235310 (2014).
- M. Sich, D. N. Krizhanovskii, M. S. Skolnick, A. V. Gorbach, R. Hartley, D. V. Skryabin, E. A. Cerdá-Mendez, K. Biermann, R. Hey, and P. V. Santos, Nat. Photon. **6**, 50 (2012).
- I. Carusotto and C. Ciuti, Rev. Mod. Phys. **85**, 299 (2013).
- A. Amo, J. Lefrère, S. Pigeon, C. Adrados, C. Ciuti, I. Carusotto, R. Houdré, E. Giacobino, and A. Bramati, Nat. Phys. **5**, 805–810 (2009).
- D. Sanvitto, F. M. Marchetti, M. H. Szymańska, G. Tosi, M. Baudisch, F. P. Laussy, D. N. Krizhanovskii, M. S. Skolnick, L. Marrucci, A. Lemaître, J. Bloch, C. Tejedor, and L. Viña, Nat. Phys. **6**, 527–533 (2010).
- V. Kohnle, Y. Léger, M. Wouters, M. Richard, M. T. Portella-Oberli, and B. Deveaud-Plédran, Phys. Rev. Lett. **106**, 255302 (2011).
- G. Li, Phys. Rev. A **93** 93, 013837 (2016).
- D. A. Zezulin, Y. V. Kartashov, D. V. Skryabin, and I. A. Shelykh, ACS Photonics **5**, 3634–3642 (2018).
- C. E. Whittaker, B. Dzurnak, O. A. Egorov, G. Buonaiuto, P. M. Walker, E. Cancellieri, D. M. Whittaker, E. Clarke, S. S. Gavrilov, M. S. Skolnick, and D. N. Krizhanovskii, Phys. Rev. X **7**, 031033 (2017).
- K. G. Lagoudakis, M. Wouters, M. Richard, A. Baas, I. Carusotto, R. André, L. S. Dang, and B. Deveaud Plédran, Nat. Phys. **4**, 706 (2008).
- K. G. Lagoudakis, T. Ostatnický, A. V. Kavokin, Y. G. Rubo, R. André, B. Deveaud-Plédran, Science **326**, 974–976 (2009).
- M. D. Fraser, G. Roumpos, and Y. Yamamoto, New J. Phys. **11**, 113048 (2009).
- G. Nardin, G. Grossi, Y. Léger, B. Piętka, F. Morier-Genoud, D. Deveaud-Plédran, Nat. Phys. **7**, 635 (2011).
- S. Pigeon, I. Carusotto, and C. Ciuti, Phys. Rev. B **83**, 144513 (2011).
- G. Grossi, G. Nardin, F. Morier-Genoud, Y. Léger, and B. Deveaud-Plédran, Phys. Rev. Lett. **107**, 245301 (2011).
- L. Dominici, R. Carretero-González, A. Gianfrate, J. Cuevas-Maraver, A. S. Rodrigues, D. J. Frantzeskakis, G. Lerario, D. Ballarini, M. De Giorgi, G. Gigli, P. G. Kevrekidis, and D. Sanvitto, Nat. Commun. **9**, 1467 (2018).
- R. Dall, M. D. Fraser, A. S. Desyatnikov, G. Li, S. Brodbeck, M. Kamp, C. Schneider, S. Höfling, and E. A. Ostrovskaya, Phys. Rev. Lett. **113**, 200404 (2014).
- T. Gao, O. A. Egorov, E. Estrecho, K. Winkler, M. Kamp, C. Schneider, S. Höfling, A. G. Truscott, and E. A. Ostrovskaya, Phys. Rev. Lett. **121**, 225302 (2018).
- X. Ma, and S. Schumacher, Phys. Rev. Lett. **121**, 227404 (2018).
- M.-S. Kwon, B. Y. Oh, S.-H. Gong, J.-H. Kim, H. K. Kang, S. Kang, J. D. Song, H. Choi, and Y.-H. Cho, Phys. Rev. Lett. **122**, 045302 (2019).
- F. M. Marchetti and M. H. Szymańska, Vortices in Polariton OPO Superfluids, in *Exciton Polaritons in Microcavities*, Springer Series in Solid-State Sciences 172, Springer-Verlag Berlin Heidelberg 2012.
- A. Gallemí, M. Guilleumas, M. Richard, and A. Minguzzi, Phys. Rev. B **98**, 104502 (2018).

28. C. W. Lai, N. Y. Kim, S. Utsunomiya, G. Roumpos, H. Deng, M. D. Fraser, T. Byrnes, P. Recher, N. Kumada, T. Fujisawa, and Y. Yamamoto, *Nature* **450**, 529–532 (2007).
29. V. G. Sala, D. D. Solnyshkov, I. Carusotto, T. Jacqmin, A. Lemaître, H. Terças, A. Nalitov, M. Abbarchi, E. Galopin, I. Sagnes, J. Bloch, G. Malpuech, and A. Amo, *Phys. Rev. X* **5**, 011034 (2015).
30. C. Schneider, K. Winkler, M. D. K. Fraser, M. Kamp, Y. Yamamoto, E. A. Ostrovskaya, S. Hofling, *Rep. Prog. Phys.* **80**, 016503 (2017).
31. G. Díaz-Camacho, C. Tejedor, and F. M. Marchetti, *Phys. Rev. B* **97**, 245309 (2018).
32. J. Yang, *Nonlinear Waves in Integrable and Non-Integrable Systems* (SIAM, 2010), Chap. 5–6.
33. L. Dominici, D. Colas, A. Gianfrate, A. Rahmani, C. Sánchez Muñoz, D. Ballarini, M. De Giorgi, G. Gigli, F. P. Laussy, and D. Sanvitto, Ultrafast topology shaping by a Rabi-oscillating vortex, arXiv:1801.02580 [cond-mat.quant-gas]

FULL REFERENCES WITH TITLES

REFERENCES

1. H. Deng, H. Haug, and Y. Yamamoto, Exciton-polariton Bose-Einstein condensation *Rev. Mod. Phys.* **82**, 1489 (2010).
2. A. Amo, S. Pigeon, D. Sunvitto, V. G. Sala, R. Hivet, I. Carusotto, F. Pisanello, G. Lemenager, R. Houdre, E. Giacobino, C. Ciuti, and A. Bramati, Polariton superfluids reveal quantum hydrodynamic solitons, *Science* **332**, 1167 (2011).
3. A. V. Yulin, O. A. Egorov, F. Lederer, and D. V. Skryabin, Dark polariton solitons in semiconductor microcavities, *Phys. Rev. A* **78**, 061801(R) (2008).
4. Y. Xue and M. Matuszewski, Creation and abrupt decay of a quasi-stationary dark soliton in a polariton condensate, *Phys. Rev. Lett.* **112**, 216401 (2014).
5. V. Goblot, H. S. Nguyen, I. Carusotto, E. Galopin, A. Lemaître, I. Sagnes, A. Amo, and J. Bloch, Phase-controlled bistability of a dark soliton train in a polariton fluid, *Phys. Rev. Lett.* **117**, 217401 (2016).
6. L. A. Smirnov, D. A. Smirnova, E. A. Ostrovskaya, and Yu. S. Kivshar, Dynamics and stability of dark solitons in exciton-polariton condensates, *Phys. Rev. B* **89**, 235310 (2014).
7. M. Sich, D. N. Krizhanovskii, M. S. Skolnick, A. V. Gorbach, R. Hartley, D. V. Skryabin, E. A. Cerda-Mendez, K. Biermann, R. Hey, and P. V. Santos, Observation of bright solitons in a semiconductor microcavity, *Nat. Photon.* **6**, 50 (2012).
8. I. Carusotto and C. Ciuti, Quantum fluids of light, *Rev. Mod. Phys.* **85**, 299 (2013).
9. A. Amo, J. Lefrère, S. Pigeon, C. Adrados, C. Ciuti, I. Carusotto, R. Houdré, E. Giacobino, and A. Bramati, Superfluidity of polaritons in semiconductor microcavities, *Nat. Phys.* **5**, 805–810 (2009).
10. D. Sanvitto, F. M. Marchetti, M. H. Szymańska, G. Tosi, M. Baudisch, F. P. Laussy, D. N. Krizhanovskii, M. S. Skolnick, L. Marrucci, A. Lemaître, J. Bloch, C. Tejedor, and L. Viña, Persistent currents and quantized vortices in a polariton superfluid, *Nat. Phys.* **6**, 527–533 (2010).
11. V. Kohnle, Y. Léger, M. Wouters, M. Richard, M. T. Portella-Oberli, and B. Deveaud-Plédran, From Single Particle to Superfluid Excitations in a Dissipative Polariton Gas, *Phys. Rev. Lett.* **106**, 255302 (2011).
12. G. Li, Azimuthons and pattern formation in annularly confined exciton-polariton Bose-Einstein condensates, *Phys. Rev. A* **93** 93, 013837 (2016).
13. D. A. Zezyulin, Y. V. Kartashov, D. V. Skryabin, and I. A. Shelykh, Spin-Orbit Coupled Polariton Condensates in a Radially Periodic Potential: Multiring Vortices and Rotating Solitons, *ACS Photonics* **5**, 3634–3642 (2018).
14. C. E. Whittaker, B. Dzurnak, O. A. Egorov, G. Buonaiuto, P. M. Walker, E. Cancellieri, D. M. Whittaker, E. Clarke, S. S. Gavrilov, M. S. Skolnick, and D. N. Krizhanovskii, Polariton pattern formation and photon statistics of the associated emission, *Phys. Rev. X* **7**, 031033 (2017).
15. K. G. Lagoudakis, M. Wouters, M. Richard, A. Baas, I. Carusotto, R. André, L. S. Dang, and B. Deveaud-Plédran, Quantized vortices in an exciton-polariton condensate, *Nat. Phys.* **4**, 706 (2008).
16. K. G. Lagoudakis, T. Ostatnický, A. V. Kavokin, Y. G. Rubo, R. André, B. Deveaud-Plédran, Observation of Half-Quantum Vortices in an Exciton-Polariton Condensate, *Science* **326**, 974–976 (2009).
17. M. D. Fraser, G. Roumpos, and Y. Yamamoto, Vortex-antivortex pair dynamics in an exciton-polariton condensate, *New J. Phys.* **11**, 113048 (2009).
18. G. Nardin, G. Grosso, Y. Léger, B. Piętka, F. Morier-Genoud, D. Deveaud-Plédran, Hydrodynamic nucleation of quantized vortex pairs in a polariton quantum fluid, *Nat. Phys.* **7**, 635 (2011).
19. S. Pigeon, I. Carusotto, and C. Ciuti, Hydrodynamic nucleation of vortices and solitons in a resonantly excited polariton superfluid, *Phys. Rev. B* **83**, 144513 (2011).
20. G. Grosso, G. Nardin, F. Morier-Genoud, Y. Léger, and B. Deveaud-Plédran, Soliton instabilities and vortex street formation in a polariton quantum fluid, *Phys. Rev. Lett.* **107**, 245301 (2011).
21. L. Dominici, R. Carretero-González, A. Gianfrate, J. Cuevas-Maraver, A. S. Rodrigues, D. J. Frantzeskakis, G. Lerario, D. Ballarini, M. De

- Giorgi, G. Gigli, P. G. Kevrekidis, and D. Sanvitto, Interactions and scattering of quantum vortices in a polariton fluid, *Nat. Commun.* **9**, 1467 (2018).
22. R. Dall, M. D. Fraser, A. S. Desyatnikov, G. Li, S. Brodbeck, M. Kamp, C. Schneider, S. Höfling, and E. A. Ostrovskaya, Creation of Orbital Angular Momentum States with Chiral Polaritonic Lenses, *Phys. Rev. Lett.* **113**, 200404 (2014).
23. T. Gao, O. A. Egorov, E. Estrecho, K. Winkler, M. Kamp, C. Schneider, S. Höfling, A. G. Truscott, and E. A. Ostrovskaya, Controlled Ordering of Topological Charges in an Exciton-Polariton Chain, *Phys. Rev. Lett.* **121**, 225302 (2018).
24. X. Ma, and S. Schumacher, Vortex Multistability and Bessel Vortices in Polariton Condensates, *Phys. Rev. Lett.* **121**, 227404 (2018).
25. M.-S. Kwon, B. Y. Oh, S.-H. Gong, J.-H. Kim, H. K. Kang, S. Kang, J. D. Song, H. Choi, and Y.-H. Cho, Direct Transfer of Light's Orbital Angular Momentum onto a Nonresonantly Excited Polariton Superfluid, *Phys. Rev. Lett.* **122**, 045302 (2019).
26. F. M. Marchetti and M. H. Szymańska, Vortices in Polariton OPO Superfluids, in *Exciton Polaritons in Microcavities*, Springer Series in Solid-State Sciences 172, Springer-Verlag Berlin Heidelberg 2012.
27. A. Gallemi, M. Guilleumas, M. Richard, and A. Minguzzi, Interaction-enhanced flow of a polariton superfluid current in a ring, *Phys. Rev. B* **98**, 104502 (2018).
28. C. W. Lai, N. Y. Kim, S. Utsunomiya, G. Roumpos, H. Deng, M. D. Fraser, T. Byrnes, P. Recher, N. Kumada, T. Fujisawa, and Y. Yamamoto, Coherent zero-state and π -state in an exciton-polariton condensate array, *Nature* **450**, 529–532 (2007).
29. V. G. Sala, D. D. Solnyshkov, I. Carusotto, T. Jacqmin, A. Lemaître, H. Terças, A. Nalitov, M. Abbarchi, E. Galopin, I. Sagnes, J. Bloch, G. Malpuech, and A. Amo, Spin-Orbit Coupling for Photons and Polaritons in Microstructures, *Phys. Rev. X* **5**, 011034 (2015).
30. C. Schneider, K. Winkler, M. D. K. Fraser, M. Kamp, Y. Yamamoto, E. A. Ostrovskaya, S. Höfling, Exciton-polariton trapping and potential landscape engineering, *Rep. Prog. Phys.* **80**, 016503 (2017).
31. G. Díaz-Camacho, C. Tejedor, and F. M. Marchetti, Spontaneous patterns in coherently driven polariton microcavities, *Phys. Rev. B* **97**, 245309 (2018).
32. J. Yang, *Nonlinear Waves in Integrable and Non-Integrable Systems* (SIAM, 2010), Chap. 5–6.
33. L. Dominici, D. Colas, A. Gianfrate, A. Rahmani, C. Sánchez Muñoz, D. Ballarini, M. De Giorgi, G. Gigli, F. P. Laussy, and D. Sanvitto, Ultra-fast topology shaping by a Rabi-oscillating vortex, arXiv:1801.02580 [cond-mat.quant-gas]